



## Anhydrous Proton Conducting Hybrid Membrane Electrolytes for High Temperature (>100°C) Proton Exchange Membrane Fuel Cells

G. Lakshminarayana,<sup>a</sup> R. Vijayaraghavan,<sup>b</sup> Masayuki Nogami,<sup>a,z</sup> and I. V. Kityk<sup>c</sup>

<sup>a</sup>Department of Materials Science and Engineering, Nagoya Institute of Technology, Showa, Nagoya, 466-8555, Japan

<sup>b</sup>Materials Division, School of Advanced Sciences, VIT University, Vellore -632 014, TN, India

<sup>c</sup>Electrical Engineering Department, Czestochowa Technological University, Alabama Armii Krajowej 17, Czestochowa, Poland

Anhydrous proton conducting hybrid membranes were prepared by the sol-gel process with trimethoxysilane (TMOS)/trimethoxypropylsilane (TMPS)/triethyl phosphate (TEP) and BMIMBF<sub>4</sub> ionic liquid as precursors. The Fourier transform infrared and NMR measurements have shown good chemical stability of these hybrid membranes. Average pore sizes and specific surface areas were investigated by the Brunauer–Emmett–Teller method. Thermogravimetric analysis and differential thermal analysis measurements confirmed that the hybrid membranes were thermally stable up to 250°C. Maximum anhydrous conductivity of  $6.4 \times 10^{-3}$  S/cm was obtained for 40 wt % ionic liquid based hybrid membrane, at 150°C, with a hydrogen permeability value of  $0.8 \times 10^{-12}$  mol/cm s Pa. © 2011 The Electrochemical Society. [DOI: 10.1149/1.3546041] All rights reserved.

Manuscript submitted August 27, 2010; revised manuscript received December 28, 2010. Published February 23, 2011.

Proton exchange membrane fuel cells (PEMFCs) are one of the most attractive energy conversion technologies for many industrial applications such as mobile telephones, distributed power generations, electric vehicles, and portable electronics.<sup>1–3</sup> Perfluorinated membranes such as Nafion are widely used in PEMFCs because of their excellent mechanical and chemical stability, as well as their good proton conductivity in sufficient-humidity conditions.<sup>4</sup> However, the stability and proton conductivity of Nafion membranes are decreased at elevated temperature and low humidity conditions due to the evaporation of water molecules from the electrolyte membrane. In addition, these materials are very expensive and possess high methanol permeability, and low operating temperature (<80°C). All these drawbacks limit the large-scale commercial application of the modern perfluorinated ionomers.

Recently, some research groups<sup>5,6</sup> have reported on humidified Nafion-silica composite membranes fabricated through sol-gel method for their application in high temperature hydrogen/oxygen proton-exchange membrane fuel cells. On the other hand, the fuel cell operation in anhydrous and intermediate (100–200°C) temperature conditions provides several benefits such as higher efficiency of energy conversion, higher CO-tolerance of PEMFC system, better water and heat management, and increased rates of reaction and diffusion. Therefore, the development of PEMFC membranes, which have high proton conductivity in anhydrous (water-free) and higher temperature conditions, has attracted much attention.<sup>7–11</sup>

In organosiloxane-based inorganic–organic hybrid membranes, inorganic component of siloxane linkages increases the thermal and chemical stabilities of the membrane, and the organic component improves the flexibility.<sup>12</sup> Hence, these hybrid membranes are expected to possess suitable properties for PEMFCs at intermediate temperatures. These hybrid materials can be fabricated by utilizing the low temperature reaction of the sol-gel process. For the preparation of silicate materials, trimethoxysilane (TMOS) is one of the most popular alkoxides. In this work, for the synthesis of organically modified silicates, TMOS and trimethoxypropylsilane (TMPS) were chosen because of their relatively rapid hydrolysis under acidic conditions. The triethyl phosphate [PO(C<sub>2</sub>H<sub>5</sub>O)<sub>3</sub>] is considered as a good proton carrier because of its efficient proton donor and acceptor transport properties.<sup>13</sup> Recently, triethyl phosphate PO (C<sub>2</sub>H<sub>5</sub>O)<sub>3</sub> was used as phosphorous dopant in phosphosilicate electrolyte membranes<sup>14–16</sup> and proton conduction was observed in these materials.

One of the various approaches used to develop anhydrous membranes was realized by replacing water as the proton solvent by a liquid that has a higher boiling point. Room temperature ionic

liquids (RTILs) have also shown much potential as a replacement for water. RTILs are organic salts with a melting point below 100°C. The chemical and physical properties of ionic liquids can be varied by carefully choosing the cation and anion from among numerous possibilities. At least one ion has a delocalized charge, and one component is organic, which prevents the formation of a stable crystal lattice. Typical RTILs have unusual properties including nonvolatility, nonflammability, wide electrochemical windows, higher ionic conductivity, and excellent thermal and chemical stability. Therefore, ionic liquids (ILs) are being investigated for a wide range of applications. One field is their utilization as electrolyte component in electrochemical devices. This includes lithium ion batteries,<sup>17–19</sup> fuel cells,<sup>20–22</sup> dye-sensitive solar cells,<sup>23–25</sup> etc. Figure 1a shows the chemical structures of all the selected silica precursors, and triethyl phosphate including [BMIMBF<sub>4</sub>] ionic liquid. Figure 1b presents the hydrolysis and condensation reactions of the silica and triethyl phosphate chemical precursors. Generally, the polymerization reactions are complex in nature due to the large number of intermediate species generated. Hence it is difficult to conclude a sol-gel reaction in a simplified manner. It is considered that under anhydrous conditions, the doped IL should interact with the phosphosilicate network, and protons can move along the interface between [PO(C<sub>2</sub>H<sub>5</sub>O)<sub>3</sub>] and ionic liquid. To confirm the interaction between the doped ionic liquid and the phosphosilicate inorganic network we performed the Fourier transform infrared (FTIR), and <sup>31</sup>P, <sup>1</sup>H, and <sup>13</sup>C MAS NMR measurements for all the prepared hybrid membranes and we observed several spectral bands shifting in the FTIR spectra, and several chemical shifts shifting in <sup>31</sup>P, <sup>1</sup>H, and <sup>13</sup>C NMR spectra of these hybrid membranes with respect to pure ionic liquid. These changes in the spectral bands and chemical shifts unambiguously confirm the interaction between the doped ionic liquid and phosphosilicate inorganic network. Previously, some other research groups<sup>26,27</sup> also reported the interaction of ionic liquid [BMIM][TFSI] with PWA based on the <sup>31</sup>P and <sup>1</sup>H MAS NMR measurements only, for their prepared organic-inorganic hybrid membrane electrolytes. We prepared the studied membranes by sol-gel process which will allow to fabricate hybrid membranes with high homogeneity at molecular scale, with the selected chemical precursors.<sup>12</sup> Further, in the studied hybrid membranes, conductivity is due to both protons liberated from triethyl phosphate and [BMIM]<sup>+</sup>, [BF<sub>4</sub>]<sup>−</sup> ionic species. Thus, the conductivity is caused not only by ionic species such as BMIM<sup>+</sup> and BF<sub>4</sub><sup>−</sup> of doped [BMIMBF<sub>4</sub>] ionic liquid but also by intermolecular proton transfer<sup>28</sup> that exist in imidazolium based ionic liquids. The proton conduction, therefore, follow a combination of Grothuss- and vehicle-type mechanisms which is confirmed by the conductivity experimental results.

<sup>z</sup> E-mail: nogami@nitech.ac.jp

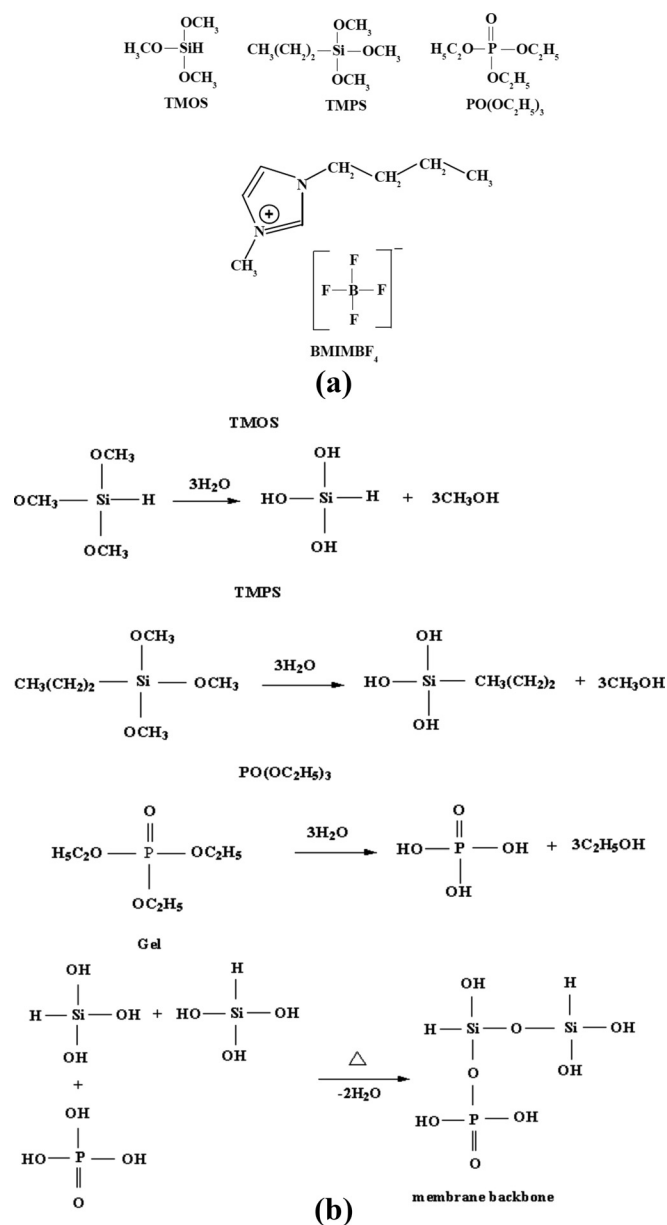


**Figure 1.** (a) Chemical structures of all the silica precursors and triethyl phosphate including [BMIMBF<sub>4</sub>] ionic liquid. (b) Hydrolysis and condensation reactions of silica precursors including trimethyl phosphate.

## Experimental

**Preparation of hybrid membranes.**—The composite membranes were prepared by using trimethoxysilane C<sub>3</sub>H<sub>10</sub>O<sub>3</sub>Si, TMOS (99%, Aldrich Chem., Co.), TMPS (97%, Aldrich Chem., Co.), triethyl phosphate [PO (C<sub>2</sub>H<sub>5</sub>O)<sub>3</sub>] (99.8%, Aldrich Chem., Co.), and [1-butyl-3-methylimidazolium tetrafluoroborate] [BMIMBF<sub>4</sub>] (99%, Aldrich Chem., Co.) ionic liquid as precursors. All the initial solvents and materials were used as received. Water purified with a Milli-Q system from Millipore (AQUARIUS/GS-20R, Japan) was used for the experiments. All the hybrids including host phosphosilicate membrane were prepared at ambient temperature under normal atmospheric pressure by sol-gel process. Several compositions of TMOS-TMPS-PO (C<sub>2</sub>H<sub>5</sub>O)<sub>3</sub>-IL (i.e., 45TMOS-45TMPS-10 PO (C<sub>2</sub>H<sub>5</sub>O)<sub>3</sub>-x [BMIMBF<sub>4</sub>] (x = 10, 20, 30, and 40 wt %) were selected for the content optimization. Here, we added [BMIMBF<sub>4</sub>] ionic liquid content in excess wt % to the host membrane 45TMOS-45TMPS-10 PO (C<sub>2</sub>H<sub>5</sub>O)<sub>3</sub> (mol %).

Initially, the calculated amount of TMOS was hydrolyzed with water (as 0.15N-HCl aq) and ethanol under stirring for 60 min at room temperature. The molar ratio of TMOS/EtOH/H<sub>2</sub>O/HCl was 1/8/4/0.01. After, TMPS which was prehydrolyzed with water (as 0.15N-HCl aq) and ethanol was added to TMOS solution under constant stirring for 60 min. The amount of TMPS was taken in equal mol ratio to TMOS. The value of *R<sub>w</sub>* (molar ratio of H<sub>2</sub>O/alkoxide) was fixed at 4 for preparation of sols. One hour later, when the above mixed solution becomes transparent, triethyl phosphate dissolved in C<sub>2</sub>H<sub>5</sub>OH with five times moles of H<sub>2</sub>O was added dropwise under magnetic stirring for 1 h. Now, the 1-butyl-3-methylimidazolium tetrafluoroborate [BMIMBF<sub>4</sub>] ionic liquid was added dropwise to the hydrolyzed solution in argon atmosphere. Keeping continuous stirring for 3 h, a homogeneous solution was formed. Finally, (N,N-dimethylformamide) HCON (CH<sub>3</sub>)<sub>2</sub> (1–3 ml) was added in standard solution followed by 60 min stirring. Such obtained clear transparent solution was called as sol. The sol was cast onto Petri dishes and gelled at 50°C for 14 days. Gel films obtained were then dried at 50°C for 6 h, and consecutively at 100°C for 6 h, 150°C for 6 h, and at 250°C for 6 h. Generally, pure ionic liquids show thermal stability up to 400°C. Therefore, we have selected the gel films heat-treatment temperature range from 50 to 250°C, in steps of 50°C increment, keeping the membranes for 6 h at each temperature. The sample thickness was varied from 0.1 to 0.5 mm. The host phosphosilicate membrane in the absence of [BMIMBF<sub>4</sub>] ionic liquid was also prepared with the same procedure as described above for comparison. The whole synthetic process is shown in Fig. 2a. The typical photograph of the 40 wt % [BMIMBF<sub>4</sub>] ionic liquid doped hybrid membrane is presented in Fig. 2b. From this photograph it is very clear that the fabricated hybrid membrane is highly transparent and mechanically stable and also still keeps a casting morphology even after drying 14 days at 50°C. The thickness of the membrane is uniform and no macrocrack and fat edge were found. Usually, in a sol-gel process, the evaporation of solvent could cause an internal stress gradient in the gel and when the stress is high enough, cracks would appear. Due to the high flexibility and processibility to make large area membranes with different thickness, these inorganic-organic membranes show an advantage over inorganic phosphosilicate materials, which require a long time to obtain thin film material by the sol-gel process.

**Characterization of membranes.**—The optical transmission spectra of all the prepared membranes were recorded by using JASCO Ubest 570 UV-vis-NIR spectrophotometer with 1 nm spectral resolution at ambient temperature within the spectral range 200–800 nm. The FTIR spectra of the composite membranes were recorded by with JASCO FTIR-460 Plus spectrometer with spectral resolution about 4 cm<sup>-1</sup>. The FTIR spectra were measured within the spectral range 4000–400 cm<sup>-1</sup> by using the KBr pellet for reference. The Brunauer–Emmett–Teller (BET) specific surface areas of all the composite membranes were determined from N<sub>2</sub> adsorption-desorption isotherms at liquid nitrogen temperature. Membranes of approximately 0.05 g were degassed at 250°C for a minimum of 6 h under vacuum before the measurement. The pore size distributions were analyzed with a Quantochrome-NOVA-1000 nitrogen gas sorption analyzer. The thermal degradation process and stability of the composites were investigated by thermogravimetric analysis, and differential thermal analysis (DTA) (Thermoplus 2, TG- 8120, Rigaku). The measurements were carried out under dry air with a heating rate of 5°C/min. The <sup>31</sup>P magic angle spinning (MAS) NMR spectra were measured with a Varian Unity Inova 300 spectrometer at 121.42 MHz with a sample spinning rate of 5000 Hz, and chemical shifts were measured with reference to 85% aqueous H<sub>3</sub>PO<sub>4</sub>. The solid state high-resolution <sup>1</sup>H and <sup>13</sup>C MAS NMR spectra were obtained by using a Varian UNITY-400 plus spectrometer at the resonance frequency of 400 MHz, respectively. The <sup>1</sup>H and <sup>13</sup>C spectra were measured by a single-pulse

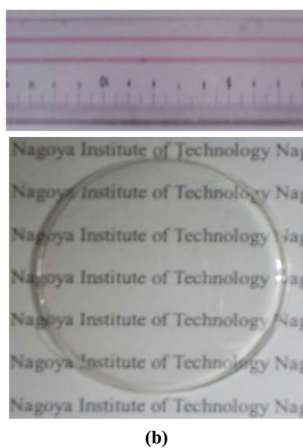
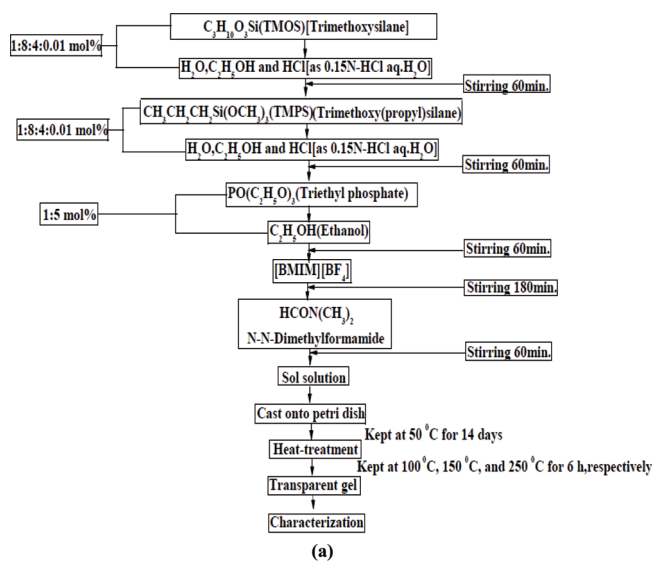


**Figure 2.** (Color online) (a) Synthetic procedure for obtaining the 45TMOS-45TMPS-10[PO(C<sub>2</sub>H<sub>5</sub>O)<sub>3</sub>]-x [BMIMBF<sub>4</sub>] (x = 10, 20, 30, and 40 wt %) hybrid membranes. (b) Photograph of the 40 wt % [BMIMBF<sub>4</sub>] ionic liquid doped hybrid membrane.

sequence, and the <sup>31</sup>P spectra were traced by a single-pulse sequence with high power <sup>1</sup>H decoupling. All the NMR measurements were performed at 25 °C. The conductivity of the membranes was measured by an ac method using Solartron SI-1260 impedance analyzer. Gold was evaporated on both sides of the membranes as electrodes, and conductivity was determined from the impedance data obtained within the frequency range from 1 to 10<sup>7</sup> Hz with signal amplitude of 10 mV. The temperature was raised stepwise and the measurements were carried out after keeping the membrane at each temperature for 1 h under dry nitrogen. Conductivities were measured within the temperature range -30–150 °C. The conductivity ( $\sigma$ ) was calculated from the electrolyte resistance ( $R$ ) obtained from the intercept of the Cole-Cole plot with the real axis, the thickness ( $l$ ) and the electrode area ( $A$ ) according to the equation  $\sigma = l/AR$ . Hydrogen permeability of the membranes (0.5 mm thick) was measured by using a forced convection drying oven (DO-600FA), under dry conditions, consisting of two compartments with a capacity of approximately 50 cm<sup>3</sup>, separated by a vertical membrane with an effective area of 20 cm<sup>2</sup>. The contents of the compartments were under constant agitation. Gas concentrations were measured by Varian CP-4900 Micro GC gas chromatography with relative standard deviation (RSD) of 0.13%.

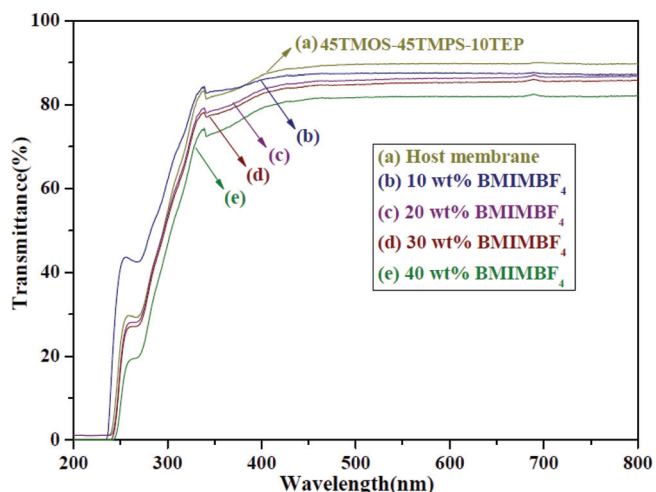


**Figure 3.** (Color online) UV-visible transmission spectra of 45TMOS-45TMPS-10[PO(C<sub>2</sub>H<sub>5</sub>O)<sub>3</sub>]-x [BMIMBF<sub>4</sub>] (x = 0, 10, 20, 30, and 40 wt %) membranes.

## Results and Discussion

Figure 3 presents the UV-visible optical transmission spectra of all the prepared composite membranes. From this figure, it is found that with ionic liquid content increment, the transmittance decreased from 89 to 82% in the prepared membranes, respectively. However, these spectra exhibit high optical transmittance value for all the membranes, i.e., above 80% at the wavelength of 800 nm. Chemical stability of electrolyte membranes is of much concern to the lifetime of PEMFCs. Figures 4a and 4b show the FTIR spectra of 45TMOS-45TMPS-10[PO(C<sub>2</sub>H<sub>5</sub>O)<sub>3</sub>] host membrane and Figs. 4c and 4d show ionic liquid doped hybrid membranes. For host matrix, spectral peaks at 456, 545, 578, 640, 795, 836, 854, 873, 1051, 1634, 2963, 3419, and 3652 cm<sup>-1</sup> are identified. It is generally known that fourfold coordinated silicon is the basic building block of the silica based glasses. Similarly, in pure P<sub>2</sub>O<sub>5</sub> glass the basic building block is the P(Q<sup>3</sup>) tetrahedron, possessing three bridging oxygens and one terminal double-bonded oxygen.<sup>29</sup> In pure SiO<sub>2</sub> glass, an increase in the coordination number of Si was observed only under high pressures above 10 GPa.<sup>30</sup> However, in phosphosilicate systems there exists a possibility of formation of sixfold coordinated silicon.<sup>29</sup> The broad absorption band centered at 1051 cm<sup>-1</sup> is assigned to  $\nu_{as}$ Si-O-Si (TO mode) vibrations. Generally, in silica matrices the spectral bands within the 1960–1640 cm<sup>-1</sup> wavenumber range correspond to combination of vibrations of the SiO<sub>2</sub> network (1640 cm<sup>-1</sup> band should often hidden by molecular water band). Dried gels obtained with dimethylformamide also present a shoulder around 1690 cm<sup>-1</sup> that is characteristic of a C=O band. Spectral bands within the wavenumber range 2800–3000 cm<sup>-1</sup> corresponds to the symmetric and asymmetric fundamental stretching vibrations of CH<sub>2</sub> and CH<sub>3</sub> groups belonging to alkoide and solvent residues. Further, within the wavenumber range 4000–3000 cm<sup>-1</sup>, the spectral bands should occur mainly due to overtones or combinations of vibrations of Si-O-H or H<sub>2</sub>O. A broad OH stretching band with weak intensity has also found within the spectral range 3500–3750 cm<sup>-1</sup>. The small spectral band appeared around 3419 cm<sup>-1</sup>, is assigned to silanol groups linked to molecular water through hydrogen bonds. The spectral bands within the wavenumber range 400–880 cm<sup>-1</sup> are attributed to the Si-O-Si bond bending vibrations and symmetric stretching vibrations of Si-O-Si bonds, respectively.<sup>12,31,32</sup> In the selected phosphosilicate matrix, the IR absorption band appeared at 873 cm<sup>-1</sup> is assigned to P-O-P asymmetric stretching mode. Spectral band centered at 795 cm<sup>-1</sup> is due to the symmetric stretching of the P-O-P and Si-O-Si (bridging oxygen atoms between the tetrahedral) bonds. Within the wavenumber range 400–4000 cm<sup>-1</sup> several spectral bands are identified for

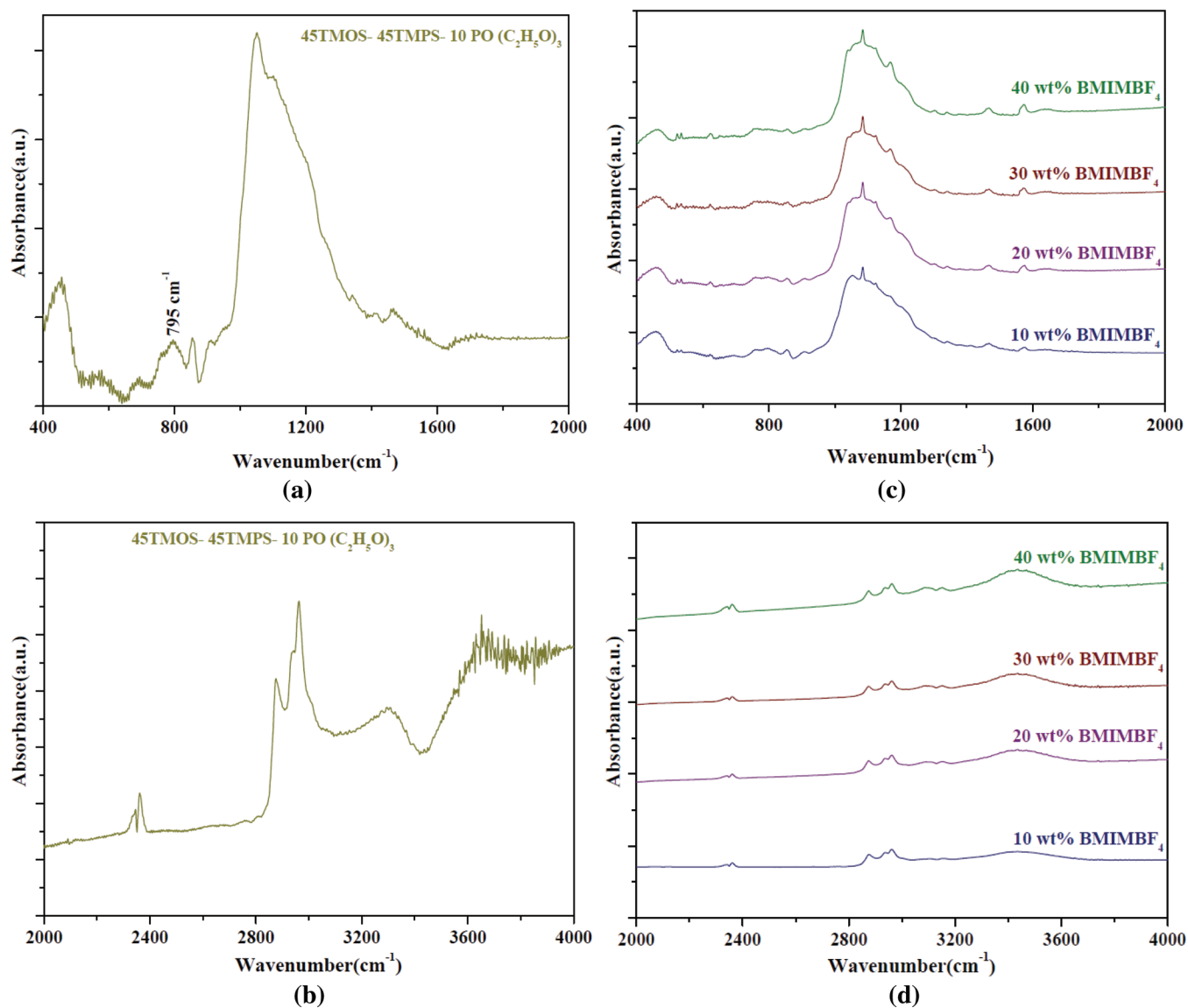


**Figure 4.** (Color online) FTIR spectra of (a), (b) 45TMOS-45TMPS-10[PO(C<sub>2</sub>H<sub>5</sub>O)<sub>3</sub>] host membrane and (c), (d) ionic liquid doped hybrid membranes.

45TMOS-45TMPS-10 PO (C<sub>2</sub>H<sub>5</sub>O)<sub>3</sub> (mol %) membranes doped with 10–40 wt % [BMIMBF<sub>4</sub>] ionic liquid. All these observed bands correlate well with the pure [BMIMBF<sub>4</sub>] ionic liquid spectral bands.<sup>31,32</sup> It should be emphasized that all the phosphosilicate matrices related spectral bands within the wavenumber range 400–1200 cm<sup>-1</sup> are overlapped well with ionic liquid related spectral bands. According to previous study, multiple hydrogen bonds should be formed between the alkyl C–H and ring C–H of BMIM<sup>+</sup> and BF<sub>4</sub><sup>-</sup> anions.<sup>33</sup> The alkyl C–H and ring C–H stretching modes supply valuable spectroscopic information for the study of hydrogen bond interactions in ILs.<sup>34</sup> The intensity of asymmetric stretching vibrations BF<sub>4</sub><sup>-</sup> (1084 cm<sup>-1</sup>) becomes stronger in the hybrid membranes with the ionic liquid weight ratio increment.

NMR spectroscopic techniques can be used to study ionic interactions and ionic states. Figure 5 shows (a) <sup>31</sup>P, (b) <sup>1</sup>H, and (c) <sup>13</sup>C MAS NMR spectra of all the prepared hybrid membranes, respectively. From the <sup>31</sup>P MAS NMR spectra (Fig. 5a), a peak at 2.5 ppm is found for host phosphosilicate matrix which is assigned to the isolated phosphorus content (Q<sup>0</sup> unit). For 10–40 wt % [BMIMBF<sub>4</sub>] ionic liquid doped hybrid membranes, this peak (Q<sup>0</sup> unit) is observed at 2.4, 2.3, 2.1, and 2.0 ppm, respectively. For all the IL doped hybrid membranes, the shifting of Q<sup>0</sup> unit compared with

host phosphosilicate membrane indicates the interaction of ionic liquid with phosphosilicate network. From Fig. 5b, <sup>1</sup>H chemical shifts at 8.8, 7.6, 4.3, 3.9, 3.3, 1.9, 1.3, and 1.0 ppm are observed for 10 wt % ionic liquid doped hybrid membrane, while for 40 wt % IL doped hybrid, signals at 8.6, 7.5, 4.2, 3.8, 3.1, 1.7, 1.2, and 0.7 ppm are identified. In IL doped hybrids, several <sup>1</sup>H chemical shifts are shifted compared with pure ionic liquid [8.4 (s, 1H, NCHN), 7.4 (s, 1H, CH<sub>3</sub>NCHCHN), 7.3 (s, 1H, CH<sub>3</sub>NCHCHN), 4.0 (t, 2H, *J* = 7.3 Hz, NCH<sub>2</sub>(CH<sub>2</sub>)<sub>2</sub>CH<sub>3</sub>), 3.7 (s, 3H, NCH<sub>3</sub>), 1.6 (quintet, 2H, *J* = 7.4 Hz, NCH<sub>2</sub>CH<sub>2</sub>CH<sub>2</sub>CH<sub>3</sub>), 1.0 [sextet, 2H, *J* = 7.3 Hz, N(CH<sub>2</sub>)<sub>2</sub>CH<sub>2</sub>CH<sub>3</sub>], and 0.6 [t, 3H, *J* = 7.3 Hz, N(CH<sub>2</sub>)<sub>3</sub>CH<sub>3</sub>]<sup>32</sup> due to the interaction between phosphosilicate content and doped ionic liquid. The chemical shifts in NMR spectra can be used to investigate the interaction between anions and cations, because they are affected by electron cloud density. The interaction between anions and cations in ionic liquid should be changed when phosphosilicate content is added to BMIMBF<sub>4</sub> through the sol-gel process. In pure BMIMBF<sub>4</sub> ionic liquid, anion and cation attract with each other by coulombic interactions. Further, H<sub>2</sub>(NCHN), H<sub>4</sub>(CH<sub>3</sub>NCHCHN), and H<sub>5</sub>(CH<sub>3</sub>NCHCHN) of ionic liquid cation should form weak hydrogen bonds with the fluorine atoms of ionic liquid anion. The chemical shifts of NCHN, CH<sub>3</sub>NCHCHN, and CH<sub>3</sub>NCHCHN from

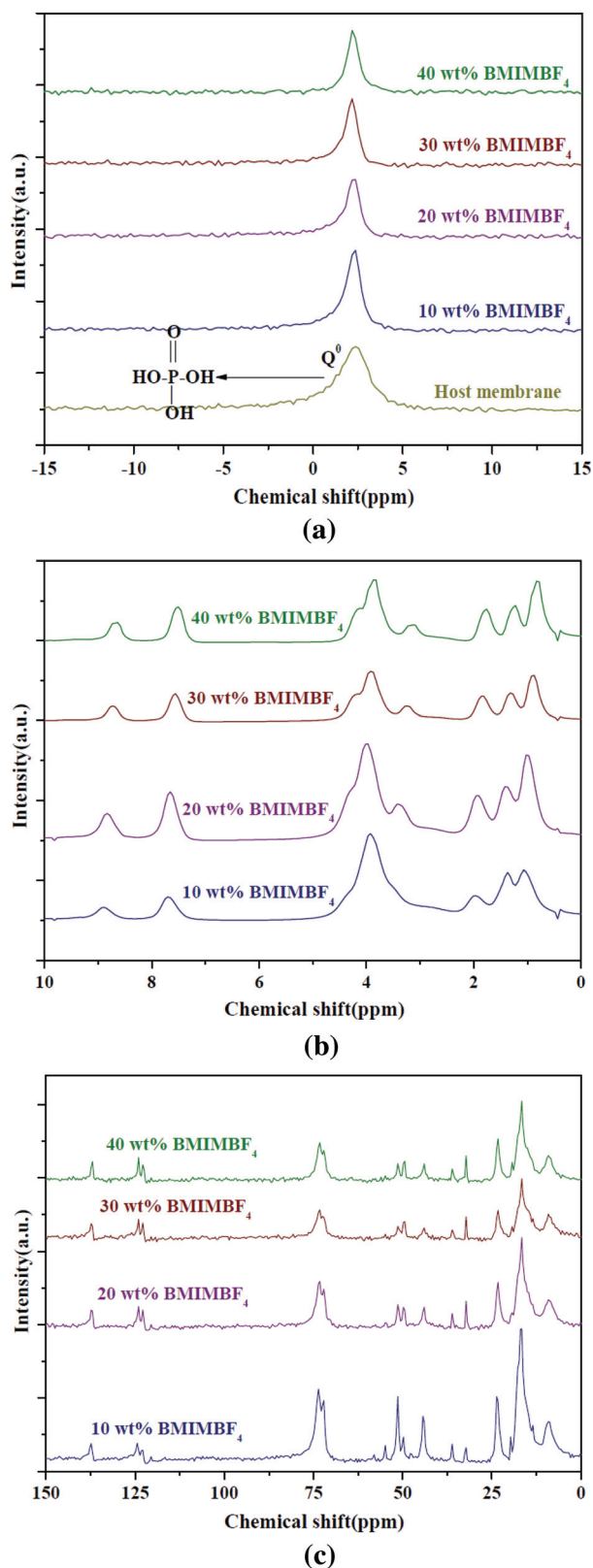


**Figure 5.** (Color online) (a)  $^{31}\text{P}$ , (b)  $^1\text{H}$ , and (c)  $^{13}\text{C}$  MAS NMR spectra for 45TMOS-45TMPS-10[PO(C<sub>2</sub>H<sub>5</sub>O)<sub>3</sub>]-x [BMIMBF<sub>4</sub>] (x = 0, 10, 20, 30, and 40 wt %) composite membranes.

cations undergo the influence between anion and inorganic phosphosilicate content. Among these hydrogen atoms, H2 is highly sensitive due to its location between two highly electronegative nitrogen atoms. The electron cloud density around H2 is small, and the

acidity is large. Inorganic phosphosilicate content may also establish hydrogen bonds with tetrafluoroborate anion, and hence BF<sub>4</sub><sup>-</sup> may far away or approach to BMIM<sup>+</sup> cation. Further, from the  $^{13}\text{C}$  NMR spectra, for 10 and 40 wt % IL doped hybrid membranes (Fig. 5c), chemical shifts at [137.4, 124.4, 122.8, 120.5, 73.4, 72.2, 55.0, 51.2, 49.7, 47.6, 44.3, 36.1, 32.2, 23.6, 16.9, and 9.0 ppm]; and [136.9, 124.1, 122.5, 73.2, 72.2, 51.2, 49.4, 43.8, 36.1, 32.2, 23.3, 16.7, and 8.7 ppm] are found, respectively. With ionic liquid content increment the chemical shifts intensity within the range 75–40 ppm is decreased gradually while the signal intensity at 32 ppm is increased. Compared with pure ionic liquid  $^{13}\text{C}$  NMR signals {136.5(NCHN), 123.3(CH<sub>3</sub>NCHCHN), 122.0(CH<sub>3</sub>NCHCHN), 48.9[N(CH<sub>2</sub>(CH<sub>2</sub>)<sub>2</sub>CH<sub>3</sub>), 35.3(NCH<sub>3</sub>), 31.5(NCH<sub>2</sub>CH<sub>2</sub>CH<sub>2</sub>CH<sub>3</sub>), 18.8 [N(CH<sub>2</sub>)<sub>2</sub>CH<sub>2</sub>CH<sub>3</sub>], and 12.6[N(CH<sub>2</sub>)<sub>3</sub>CH<sub>3</sub>] ppm}<sup>32</sup> the shifting of  $^{13}\text{C}$  NMR signals suggests the interaction of ionic liquid with inorganic phosphosilicate content.

For all the prepared membranes, specific surface areas and pore-size distributions are determined from nitrogen adsorption/desorption isotherms (see figure provided in the supplemental data<sup>47</sup>). Table I shows the pore size and surface area features of all the membranes. The BET surface areas of the membranes along with their average pore diameters were evaluated following the BET method and reported in the Table I. The pore size distribution was calculated as a function of volume or specific surface area of the pores. Following Table I, it is confirmed that all such fabricated ionic liquid doped hybrid membranes do not possess a porous structure and surface areas are calculated to be lower than 0.5 m<sup>2</sup>/g. This result suggests that the IL doped hybrids were dense in structure. This should be due to a fact that the doped ionic liquid has filled in the porous structure of the inorganic phosphosilicate network.<sup>32</sup> This was also confirmed by the conductivity measurements, discussed later. The enhancement in the conductivity of ionic liquid doped phosphosilicate membranes occur by ionic liquid absorption into the existing pores. Here the ionic liquid molecules provide a bulk transport mechanism for the charge carrying protons within the membrane.

It is necessary to investigate the thermal stability of PEMs because a medium temperature operation (<100°C) is aimed for the prepared hybrid membranes. Thermal properties of all the prepared membranes are investigated by both thermogravimetry (TG) and DTA, respectively. Figures 6a and 6b show the TG and DTA profiles of all the prepared membranes. An initial loss, 3 wt % was found at 80°C for host matrix. This first weight loss region below 100°C is due to the evaporation of physical weakly and chemically strongly bound water molecules. 7 and 10 wt % losses were observed around at 400 and 460°C due to the condensation of structural hydroxyl groups, respectively. Generally, glasses fabricated by sol-gel processes contain a certain amount of water molecules in them. These H<sub>2</sub>O molecules in the gel exist such as physically adsorbed water molecules in the pores, bound in the pore surface SiOH groups, surface OH groups bonded to Si ions, OH bonds surrounded with SiO<sub>4</sub> tetrahedral silica networks,<sup>12</sup> etc. The observed weight loss of all the IL doped membranes below 100°C was 2.0 wt % only due to the high amount of added ionic liquid. The hybrid membranes studied in the present work are found to be thermally

**Table I.** Textural properties of 45TMOS-45TMPS-10[PO(C<sub>2</sub>H<sub>5</sub>O)<sub>3</sub>]-x [BMIMBF<sub>4</sub>] (x = 0, 10, 20, 30, and 40 wt %) membranes.

Sample	Composition of TMOS-TMPS-[PO(C <sub>2</sub> H <sub>5</sub> O) <sub>3</sub> ]-[BMIMBF <sub>4</sub> ]	Average pore size (nm)	Average pore volume (cm <sup>3</sup> /g)	Specific surface area (m <sup>2</sup> /g)
A1	(45-45-10)-0 wt %	2.613	0.093	142
A2	(45-45-10)-10 wt %	No pores	~0	< 0.5
A3	(45-45-10)-20 wt %	No pores	~0	<0.5
A4	(45-45-10)-30 wt %	No pores	~0	<0.5
A5	(45-45-10)-40 wt %	No pores	~0	<0.5

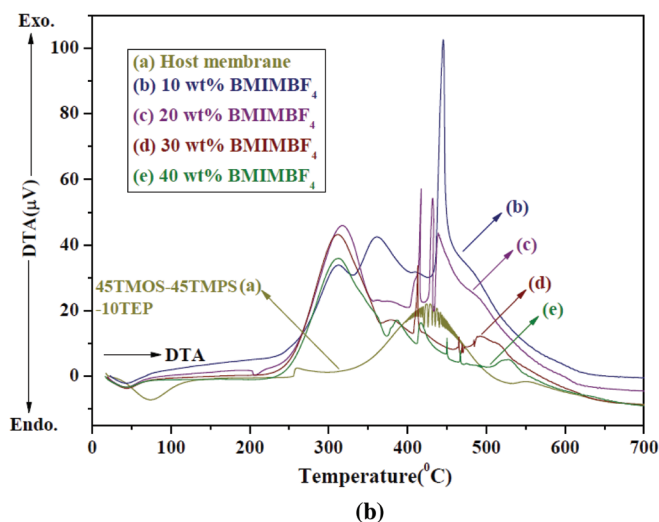
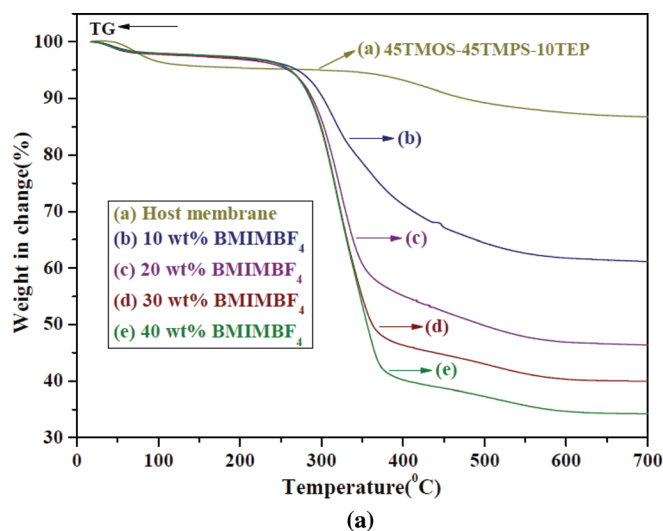


**Figure 6.** (Color online) (a) TG and (b) DTA profiles of 45TMOS-45TMPS-10[PO(C<sub>2</sub>H<sub>5</sub>O)<sub>3</sub>]-x [BMIMBF<sub>4</sub>] (x = 0, 10, 20, 30, and 40 wt %) membranes.

stable up to temperatures of 250°C and can be used at temperatures within the 100–200°C range for PEMFCs. Following the host matrix DTA profile, exothermic peaks at 260, 426, and 553°C are identified, including one endothermic peak at 74°C. All these exothermic peaks indicates the decomposition or burning of the residual organic groups in the phosphosilicate matrix. For 10–40 wt % IL doped membranes, exothermic peaks at 312, 362, 413, 445, and 487°C; 317, 418, 432, 440, and 490°C; 311, 382, 413, 466, and 504°C; and 313, 388, 417, 450, 467, and 528°C are found. These peaks suggest the decomposition of the doped IL. Also, from the all IL doped membranes one endothermic peak at 43°C was observed.

Figure 7 presents the Cole-Cole representation of impedance data (80–150°C) measured for 40 wt % [BMIMBF<sub>4</sub>] ionic liquid based hybrid membrane. For more clarity about resistance of the membranes, we have provided an inset to Fig. 7 considering the high frequency region of the impedance curves. Under anhydrous conditions, the Cole-Cole plots showed the semicircle component at high frequencies. The semicircle at high frequency was explained with the capacitive behavior of the interface between electrodes and electrolyte. However, this component has decreased with the increase of membrane conductivity. The high frequency arc corresponds to the bulk component and low frequency arc to electrode response. The impedance spectra can be fitted with a series of three

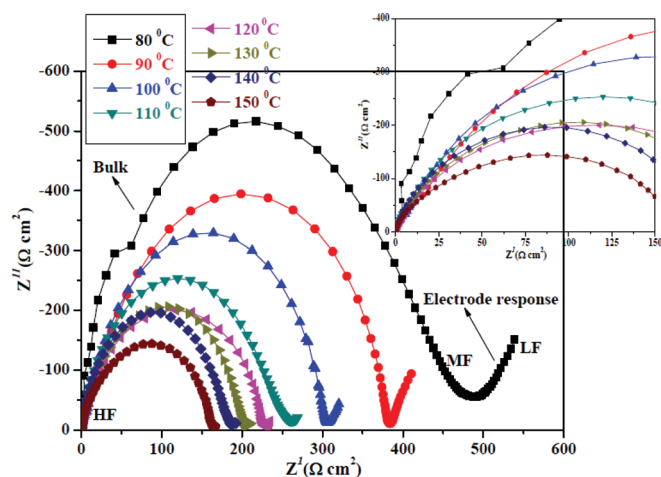


**Figure 7.** (Color online) Cole-Cole representation of impedance data (80–150°C) measured for 40 wt % [BMIMBF<sub>4</sub>] ionic liquid based hybrid membrane. Inset: high frequency region of the membrane.

electrical circuits, having resistance and constant phase element coupled in parallel. Because of depression of the arcs in some cases, the use of simple capacitor is not sufficient to model the electrical response of the materials so more complex equivalent circuit with frequency-dependent elements such as constant phase elements can be used to fit results. In the impedance spectra showing just one arc, it may be considered that the intercept on the real axis ( $Z'$ ) corresponds to the bulk resistance and the arc diameter, the interfacial resistance. Therefore, the resistances of the composite materials can be estimated from the intersection of the real axis and the linear part of the impedance spectra.<sup>12</sup>

In PEMFCs or direct methanol fuel cell (DMFCs), proton conductivity of membranes is a crucial parameter because the cell performance is strongly dependent on this property. Figure 8 shows the anhydrous conductivity of all the IL doped membranes, measured within the temperature range –30 to 150°C. For comparison, anhydrous conductivity of host phosphosilicate matrix from 20–80°C is also shown. The thickness of all the prepared hybrid membranes for the conductivity measurements was about 0.2 mm. In literature, it was reported that for Nafion membrane conductivity and permeability are in principle, thickness-independent transport parameters, although a parallel, thickness-dependent pathway is utilized in the case of facilitated transport of alkenes in silver-exchanged Nafion.<sup>35</sup>

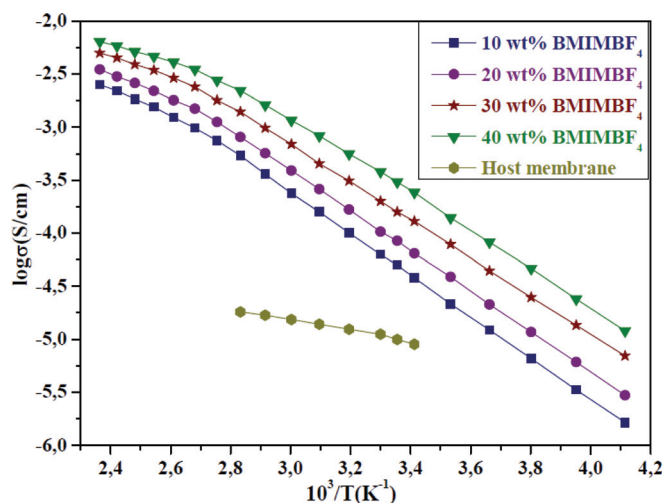


**Figure 8.** (Color online) Conductivity of 45TMOS-45TMPS-10[PO(C<sub>2</sub>H<sub>5</sub>O)<sub>3</sub>]-x [BMIMBF<sub>4</sub>] (x = 0, 10, 20, 30, and 40 wt %) membranes.

In addition, Nafion conductivity was reported to be the same for all thicknesses.<sup>36</sup> Further, recently some research groups<sup>37,38</sup> were also reported that the conductivity of the Nafion membrane was decreases with membrane thickness decrement. The measured anhydrous conductivity of host matrix at 80°C was  $1.82 \times 10^{-5}$  S/cm. This low value should be due to the loss of water molecules that exist within the membrane. On the other hand, for all the IL doped hybrid membranes the conductivity values were enhanced proportionally with 10–40 wt % IL addition. Anhydrous conductivity of  $6.4 \times 10^{-3}$  S/cm at 150°C was achieved for 40 wt % IL doped membrane. At 80°C, the 40 wt % IL doped membrane has shown conductivity value of  $2.2 \times 10^{-3}$  S/cm which is two orders of magnitude higher than that of host matrix conductivity. Generally, in PEMFCs the conductivity increment by ionic liquid doping can be explained as  $\sigma = nq\mu$ , where  $n$  is the number of free charge carriers,  $q$  is the coulombic charge, and  $\mu$  is the mobility. Further, the change in conductivity ( $\sigma$ ) is governed by changing either  $n$  or  $\mu$ , respectively. Also, the mobility ( $\mu$ ) can be expressed as  $\mu = q/6\pi\eta r$ , where  $\eta$  is viscosity. This clearly indicates that a decrease in viscosity leads to an increase in the mobility or ionic conductivity.<sup>39,40,41</sup> In our present study, for the tetrafluoroborate anion, the highly electronegative fluorine atom should be caused to the distribution of the anionic charge of borate. Also, the effect of the surface covering of the anion backbone by these fluorine atoms could be a considerable reason for weak interaction with the [BMIM]<sup>+</sup> cation. Also, in ionic liquids like BMIMBF<sub>4</sub> the C–H bonds of imidazolium cations are highly sensitive to the chemical environment, which induces strong acidity, ion-pair formation and decomposition.<sup>32,42</sup> Further, [BMIm]<sup>+</sup> should change its shape more easily than BF<sub>4</sub><sup>-</sup> due to its bigger ion radius. Following Fig. 8, one can see that the plots of anhydrous conductivity ( $\sigma$ ) versus reciprocal temperature ( $T^{-1}$ ) are not linear within the temperature range –30–150°C for the IL doped membranes, indicating both Arrhenius-type and Vogel–Tamman–Fulcher (VTF) type behavior, respectively.

The temperature dependence of the conductivity in PEMFC can be taken as an indication for a particular type of conduction mechanism. Previously, it was reported that  $\log \sigma$  versus  $1/T$  plots obey one of the following types of behavior: (1) VTF behavior throughout the studied temperature range. (2) Arrhenius behavior at low temperatures and VTF behavior at high temperature. (3) Arrhenius behavior with two activation energies. (4) VTF at low temperatures and Arrhenius behavior at high temperatures. (5) behavior which cannot be explained by either VTF nor Arrhenius.<sup>43,44</sup> The activation energy  $E_a$  which is the minimum energy required for charge transfer from one free-site to another, can be obtained for each membrane from the slope of  $\log \sigma$  vs  $T^{-1}$  plots obeying the relationship

$$\sigma = \sigma_0 e^{-(E_a/RT)} \quad [1]$$

In Eq. (1),  $\sigma$  is the conductivity (in S/cm),  $\sigma_0$  is the preexponential factor,  $E_a$  is the activation energy (in kJ/mol),  $R$  is the universal gas constant ( $=8.314$  J/mol K), and  $T$  is the absolute temperature (K). The calculated activation energies (in eV) for 10–40 wt % ionic liquid doped membranes are 0.387, 0.372, 0.360, and 0.327, respectively. The calculated value for host membrane ( $E_a = 0.093$  eV) is not really reliable as the conductivity is measured for a limited temperature range. In general, activation energy decreases with an increase in conductivity which is also observed in our present study. Gas permeability of a PEM and its impact on fuel cell operation is an important parameter that needs to be characterized under different, realistic conditions for use in the development and advancement of PEM fuel cells. When different concentrations of hydrogen or oxygen gas exist across a gas permeable membrane, the gases permeate through the membrane due to the partial pressure gradient. Figure 9 presents the measured hydrogen permeability values for 40 wt % IL doped membrane within the temperature range 20–150°C (thickness = 0.5 mm). The hydrogen permeability value was decreased from  $1.65 \times 10^{-11}$  to  $0.8 \times 10^{-12}$  mol/cm s Pa with the

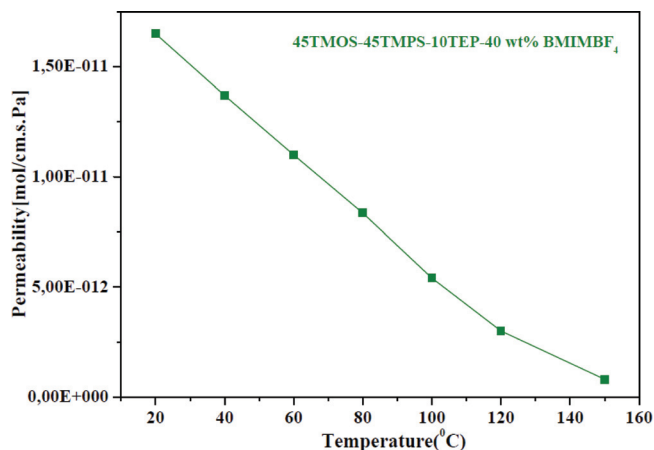


**Figure 9.** (Color online) Hydrogen permeation rate as a function of temperature for 40 wt % [BMIMBF<sub>4</sub>] doped 45TMOS–45TMPS–10[PO (C<sub>2</sub>H<sub>5</sub>O)<sub>3</sub>] (mol %) hybrid membrane (thickness = 0.5 mm). The permeability measurements were performed under hydrogen feed in the temperature range 20–150°C.

temperature increment from 20 to 150°C. Previously, it is reported that surface diffusion plays only a minor role (<2%) on the total transport mechanism in phosphosilicate materials.<sup>45</sup> Surface diffusion usually occurs simultaneously with other transport mechanisms such as Knudsen diffusion. Knudsen diffusion is prevailing when the mean free path of the gas molecules is greater than the pore size. Generally, in phosphosilicate matrices Knudsen diffusion process is responsible for the H<sub>2</sub> gas permeation decrement as the temperature increases.<sup>46</sup> However, from the BET data (Table I) of the ionic liquid doped hybrid membranes, no porous structure was observed for all these membranes confirming their relatively dense structure. The possible influence of solubility of H<sub>2</sub> gas in the ionic liquid medium would be one of the more probable causes for the observed transport behavior of hybrid membrane. The decrease of permeability with increasing temperature could be related to a decrease of the H<sub>2</sub> solubility. However the hydrogen permeability feature of ionic liquids doped inorganic-organic hybrid membranes required deeper investigations and will a subject of our future work. It is well known that the permeability coefficient of any pure gas through a membrane is directly related to the dimensions (size and thickness etc.) of the membrane including applied gas pressure. In the present work, it is possible by the selected sol-gel method to fabricate thin membranes with desired thickness just by varying the volume of sol solutions of the studied membranes, in the Petri dishes. To increase the power density, decrease of the membrane resistance by means of reduction of the thickness of the electrolyte membrane is required without loss of mechanical strength.

## Conclusions

By sol-gel synthesis, novel 1-butyl-3 methylimidazolium tetrafluoroborate ionic liquid based membrane electrolytes were prepared using trimethoxysilane, trimethoxypropylsilane, and triethyl phosphate. For all the prepared hybrid membranes, the interaction between the doped “hydrophilic” [BMIMBF<sub>4</sub>] ionic liquid and the inorganic phosphosilicate network was investigated by Fourier transform infrared spectroscopy and <sup>31</sup>P, <sup>1</sup>H, and <sup>13</sup>C MAS NMR measurements. Several spectral bands shifting in FTIR spectra, and chemical shifts shifting in <sup>31</sup>P, <sup>1</sup>H, and <sup>13</sup>C NMR spectra of these hybrid membranes compared with pure ionic liquid confirmed the interaction of doped ionic liquid and inorganic phosphosilicate network at molecular scale. The textural properties were investigated from nitrogen adsorption-desorption analysis. No pore structure was found for ionic liquid based hybrid membranes by Barrett–Joyner–Halenda desorption method that confirmed the dense structure of fabricated hybrids. The IL doped membranes show good chemical

stability and are thermally stable up to 250°C in air due to inorganic phosphosilicate network and stable tetrafluoroborate anion. The fabricated flexible, transparent, and homogenous hybrid membranes have shown good conductivity under nonhumidified conditions. Maximum anhydrous conductivity of  $6.4 \times 10^{-3}$  S/cm at 150°C was achieved for 40 wt % ionic liquid doped hybrid membrane. The conductivity of the ionic liquid doped hybrid membranes was remained stable up to 10 h during the measurements. The hydrogen permeability values were decreased from  $1.65 \times 10^{-11}$  to  $0.8 \times 10^{-12}$  mol/cm s Pa for 40 wt % IL based hybrid membrane, as the temperature increases from 20 to 150°C. These hybrid membranes can be promising materials for medium temperature (100–200°C) fuel cell electrolytes and show good processibility for large area membrane.

### Acknowledgments

The authors are grateful to the New Energy and Industrial Technology Development Organization (NEDO), Japan for the financial support.

Nagoya Institute of Technology assisted in meeting the publication costs of this article.

### References

- W. Vielstich, in *Handbook of Fuel Cells—Fundamentals, Technology and Applications*, Vol. 1, W. Vielstich, A. Lamm, and H. A. Gasteiger, Editors, p 26, Wiley, Chichester (2003).
- S. D. Mikhailenko, K. P. Wang, S. Kaliaguine, P. X. Xing, G. P. Robertson, and M. D. Guiver, *J. Membr. Sci.*, **233**, 93 (2004).
- S. J. Hamrock, and M. A. Yandrasits, *J. Macromol. Sci., Polym. Rev.*, **46**, 219 (2006).
- K. A. Mauritz and R. B. Moore, *Chem. Rev.*, **104**, 4535–4586 (2004).
- K. T. Adjemian, S. Srinivasan, J. Benziger, and A. B. Bocarsly, *J. Power Sources*, **109**, 356 (2002).
- A. K. Sahu, G. Selvarani, S. Pitchumani, P. Sridhar, and A. K. Shukla, *J. Electrochem. Soc.*, **154**, B123 (2007).
- M. L. Di Vona, A. D'Epifanio, D. Marani, M. Trombetta, E. Traversa, and S. Licoccia, *J. Membr. Sci.*, **279**, 186 (2006).
- Y. W. Kim, J. T. Park, J. H. Koh, D. K. Roh, and J. H. Kim, *J. Membr. Sci.*, **325**, 319 (2008).
- F. J. Jiang, H. T. Pu, W. H. Meyer, Y. Guan, and D. C. Wan, *Electrochim. Acta*, **53**, 4495 (2008).
- M. Q. Li and K. Scott, *Electrochem. Solid-State Lett.*, **12**, B171 (2009).
- H. T. Pu, Y. J. Qin, L. M. Tang, X. R. Teng, and Z. H. Chang, *Electrochim. Acta*, **54**, 2603 (2009).
- G. Lakshminarayana and M. Nogami, *Electrochim. Acta*, **55**, 1160 (2010).
- A. Matsuda, T. Kanzaki, M. Tatsumisago, and T. Minami, *Solid State Ionics*, **145**, 161 (2001).
- F. Damay, and L. C. Klein, *Solid State Ionics*, 162–163, 261 (2003).
- M. Aparicio and L. C. Klein, *J. Sol-Gel Sci. Technol.*, **28**, 199 (2003).
- Y. Nishiyama, S. Tanaka, H. W. Hillhouse, N. Nishiyama, Y. Egashira, and K. Ueyama, *Langmuir*, **22**, 9469 (2006).
- J. Saint, A. S. Best, A. F. Hollenkamp, J. Kerr, J. H. Shin, and M. M. Doeff, *J. Electrochem. Soc.*, **155**, A172 (2008).
- H. Sakaebe, H. Matsumoto, and K. Tatsumi, *Electrochim. Acta*, **53**, 1048 (2007).
- J. H. Shin, W. A. Henderson, C. Tizzani, S. Passerini, S. S. Jeong, and K. W. Kim, *J. Electrochem. Soc.*, **153**, A1649 (2006).
- P. Judeinstein, C. Iojoiu, J. Y. Sanchez, and B. Ancian, *J. Phys. Chem. B*, **112**, 3680 (2008).
- R. Hagiwara, T. Nohira, K. Matsumoto, and Y. Tamba, *Electrochem. Solid-State Lett.*, **8**, A231 (2005).
- C. Schmidt, T. Glück, and G. Schmidt-Naake, *Chem. Eng. Technol.*, **31**, 13 (2008).
- M. Wang, X. Xiao, X. Zhou, X. Li, and Y. Lin, *Solar Energy Mater. Solar Cells*, **91**, 785 (2007).
- D. B. Kuang, P. Wang, S. Ito, S. M. Zakeeruddin, and M. Grätzel, *J. Am. Chem. Soc.*, **128**, 7732 (2006).
- R. Kawano, H. Matsui, C. Matsuyama, A. Sato, M. A. B. H. Susan, N. Tanabe, and M. Watanabe, *J. Photochem. Photobiol., A*, **164**, 87 (2004).
- J.-D. Kim, S. Hayashi, T. Mori, and I. Honma, *Electrochim. Acta*, **53**, 963 (2007).
- J.-D. Kim, S. Hayashi, M. Onoda, A. Sato, C. Nishimura, T. Mori, and I. Honma, *Electrochim. Acta*, **53**, 7638 (2008).
- K. D. Kreuer, A. Fuchs, M. Ise, M. Spaeth, and J. Maier, *Electrochim. Acta*, **43**, 1281 (1998).
- D. Miyabe, M. Takahashi, Y. Tokuda, T. Yoko, and T. Uchino, *Phys. Rev. B*, **71**, 172202 (2005).
- C. Meade, R. J. Hemley, and H. K. Mao, *Phys. Rev. Lett.*, **69**, 1387 (1992).
- G. Lakshminarayana, V. S. Tripathi, I. Tiwari, and M. Nogami, *Ionics*, **16**, 385 (2010).
- G. Lakshminarayana and M. Nogami, *Solid State Ionics*, **181**, 760 (2010).
- S. A. Katsyuba, E. E. Zvereva, A. Vidis, and P. J. Dyson, *J. Phys. Chem. A*, **111**, 352 (2007).
- H. C. Chang, J. C. Jiang, C. Y. Chang, J. C. Su, C. H. Hung, Y. C. Liou, and S. H. Lin, *J. Phys. Chem. B*, **112**, 4351 (2008).
- R. Rabago, D. L. Bryant, C. A. Koval, and R. D. Noble, *Ind. Eng. Chem. Res.*, **35**, 1090 (1996).
- Dupont Product Information Sheet, <http://www.dupont.com/fuelcells/pdf/dfc101.pdf>, last accessed October 2009.
- S. Slade, S. A. Campbell, T. R. Ralph, and F. C. Walsh, *J. Electrochem. Soc.*, **149**, A1556 (2002).
- M. N. Tsampas, A. Pikos, S. Brosda, A. Katsaounis, and C. G. Vayenas, *Electrochim. Acta*, **51**, 2743 (2006).
- P. K. Singh and A. Chandra, *J. Phys. D*, **36**, L93 (2003).
- B. Singh and S. S. Sekhon, *Chem. Phys. Lett.*, **414**, 34 (2005).
- P. K. Singh, K. W. Kim, R. K. Nagarale, and H.-W. Rhee, *J. Phys. D*, **42**, 125101 (2009).
- P. Wassercheid, *Nature*, **439**, 797 (2006).
- M. A. Ratner, in *Polymer Electrolyte Reviews*, Vol. I, J. R. MacCallum and C. A. Vincent, Editors, Elsevier, London (1987).
- E. Morales, and J. L. Acosta, *Electrochim. Acta*, **45**, 1049 (1999).
- G. Lakshminarayana and M. Nogami, *J. Phys. Chem. C*, **113**, 14540 (2009).
- T. Uma and M. Nogami, *Chem. Mater.*, **19**, 3604 (2007).
- See supplementary material at <http://dx.doi.org/10.1149/1.3546041E-JES0AN-158-024104> for supporting figure.